# Modelling DESI Optical Corrector Distortion with Zernike Derivatives
# DESI-DOC 3105v5

Mike Lampton

August 22, 2017

## 1 Introduction

Optical distortion can be modeled with a variety of two dimensional fields. I divide this issue into two parts: the small-scale inch-size distortions that will have to be mapped with fiber rastering, and the large-scale full-field distortions that are continually monitored by our planned family of 120 fiducial lamps. Here I address only the large-scale interpolation issue.

Traditionally for this task, combinations of simple polynomials of the form $x^n y^m$ have been used. [1] [2] Recently, Steve Kent has developed an approach based on a set of orthogonal spin weighted Zernike functions and has shown excellent interpolation accuracy when modelling DESI and LSST. [3] He shows that having an orthogonal set of basis functions has two important advantages over the simple polynomial power terms: fewer terms are needed to achieve a stated accuracy, and their errors are statistically independent.

An alternative to that approach was developed by Zhao and Burge ZB07, ZB08 [4] [5] in which an orthogonal vector basis is generated from the gradients and curls of Zernike polynomials without spin weighting. The gradients themselves are not orthogonal, but no more than two polynomials per term are needed to provide the desired orthogonality.

Vector fields can be classified as to their divergence and their curl. A field with divergence=0 and curl=0 satisfies Laplace's equation. Other categories are the curl-free set with divergence, and the divergence-free group with curl.

Can the grad/curl approach work for DESI? In an earlier report, I examined using a set of 33 published ZB orthogonalized Zernike derivative vectors. I employed the procedure outlined in Figure 1, in which a best-fit DESI corrector model was generated using a reverse ray trace, either using the nominal "ideal" configuration of the optics, or a "mangled" version

[1] Ali et al, ISOCAM Field of View Distortion, ESA SP-481, 2001
[2] Anderson and King, Distortion Solution for HST WFPC2, PASP v.115 pp.113-131, 2003
[3] Kent, S., Spin-Weighted Zernike Polynomials, DESI-DOC-2763, 2017
[4] Zhao, C., and Burge, J.H., Orthonormal vector polynomials Part I, OE v.15 no. 26, 2007
[5] Zhao, C., and Burge, J.H., Orthonormal vector polynomials Part II, OE v.16 no. 9, 2008

in which the optics are seriously messed up. To evaluate the basis set, I employed the procedure shown in Figure 2, where a set of sky grid points was imaged by the DESI optical model and by the ZB model interpolation. My initial set of all 33 ZB coefficients immediately showed that about half of them have best fit coeffients that are small, the order of one part per million. Weeding these out gave a set of 12 vector fields, a subset of the potentially infinite Zhao-Burge family.

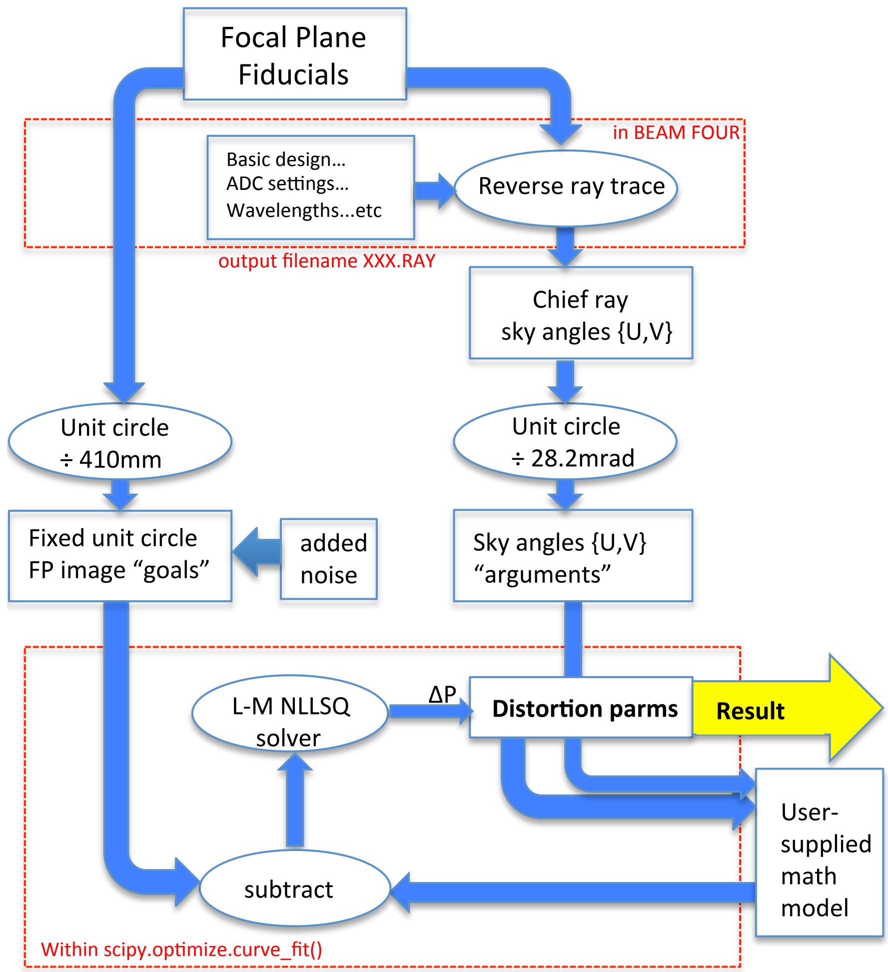


Figure 1: Flow chart for determining the best fit distortion parameters, given a set of 120 known fiducial locations and their chief ray sky angles. Calculation begins with a nominal set of 120 fiducial locations on the DESI focal surface, and their distorted sky locations are provided by a reverse ray trace having a variety of misadjustments. Python's scipy optimizer adjusts the distortion model parameters to give a best match to the known fiducials.

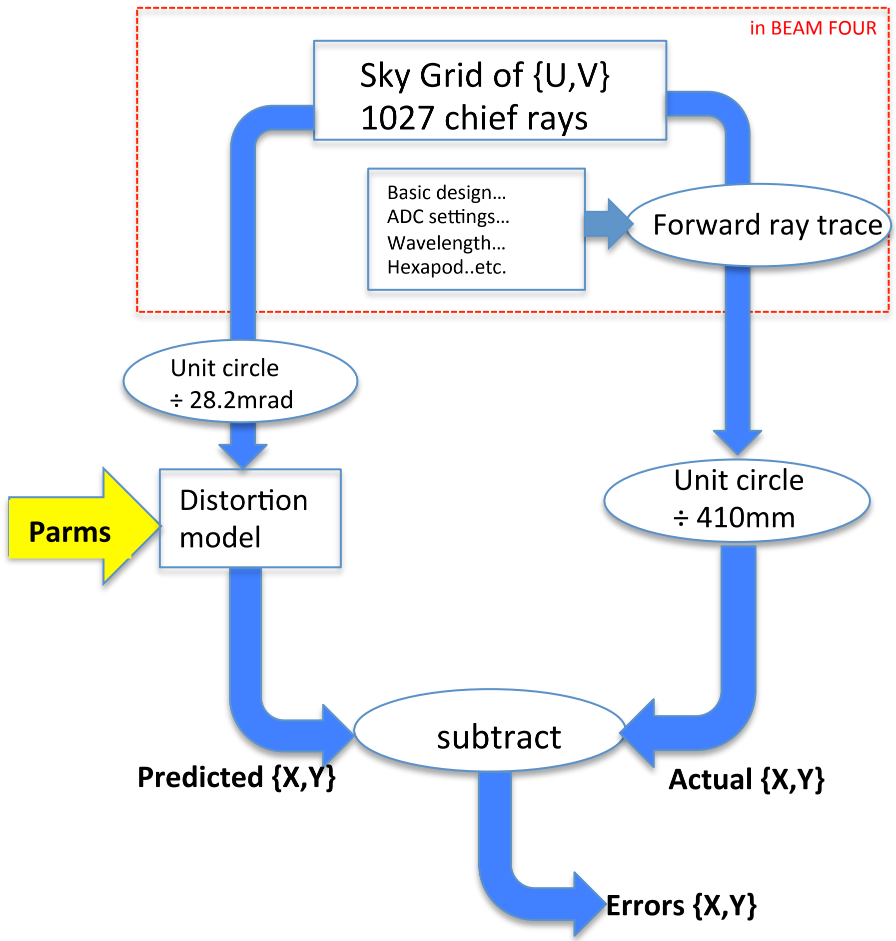


Figure 2: Flow chart for testing the distortion model and parameters. A grid of $\sim$ 1000 sky locations are forward ray traced to the focal surface, and the model predictions are compared to the ray trace. Differences reveal failures to accurately model the ray trace results.

# 2 The Polynomials

Here I restrict my attention to nine Zernike polynomials up to radial degree 6 and azimuthal index of 0 or 1. I list these nine and their sixteen orthogonalized derivatives explicitly to help maintain the audit trail. (There would be eighteen derivatives but for the fact that the lowest two curls are merely permutations of the first two gradients.) I supply a normalizing coefficient that makes the area-average dot product of any two equal to their delta function. In Figure 3 below I show how each of the sixteen fields varies over the unit circle.

**Table 1: Nine Zernike Scalar Polynomials Used Here**

| Noll | Wyant | B-W n | B-W m | Formula |
|---|---|---|---|---|
| 2 | 1 | 1 | 1 | $r * cos(t)$ |
| 3 | 2 | 1 | -1 | $r * sin(t)$ |
| 4 | 3 | 2 | 0 | $2r^2 - 1$ |
| 7 | 7 | 3 | -1 | $(3r^3 - 2r) * sin(t)$ |
| 8 | 6 | 3 | 1 | $(3r^3 - 2r) * cos(t)$ |
| 11 | 8 | 4 | 0 | $6r^4 - 6r^2 + 1$ |
| 16 | 13 | 5 | 1 | $(10r^5 - 12r^3 + 3r) * cos(t)$ |
| 17 | 14 | 5 | -1 | $(10r^5 - 12r^3 + 3r) * sin(t)$ |
| 22 | 15 | 6 | 0 | $20r^6 - 30r^4 + 12r^2 - 1$ |

**Table X: Sixteen Zernike-Derivative Fields**

| BW n, m | running | Op | Radial | Tangential | NormCoef |
|---|---|---|---|---|---|
| 1, 1 | 0 | grad | $cos(t)$ | $-sin(t)$ | 1 |
| 1, 1 | 1 | grad | $sin(t)$ | $cos(t)$ | 1 |
| 2, 0 | 2 | grad | $4r$ | 0 | $1/\sqrt{8}$ |
| 3, 1 | 3 | grad | $(9r^2 - 3)sin(t)$ | $(3r^2 - 3)cos(t)$ | $1/\sqrt{6}$ |
| 3, 1 | 4 | grad | $(9r^2 - 3)cos(t)$ | $-(3r^2 - 3)sin(t)$ | $1/\sqrt{6}$ |
| 4, 0 | 5 | grad | $(24r^3 - 16r)$ | 0 | $1/\sqrt{16}$ |
| 5, 1 | 6 | grad | $(50r^4 - 45r^2 + 5)cos(t)$ | $-(10r^4 - 15r^2 + 5)sin(t)$ | $1/\sqrt{10}$ |
| 5, 1 | 7 | grad | $(50r^4 - 45r^2 + 5)sin(t)$ | $(10r^4 - 15r^2 + 5)cos(t)$ | $1/\sqrt{10}$ |
| 6, 0 | 8 | grad | $120r^5 - 144r^3 + 36r$ | 0 | $1/\sqrt{24}$ |
| 2, 0 | 9 | curl | 0 | $-4r$ | $1/\sqrt{8}$ |
| 3, 1 | 10 | curl | $-(3r^2 - 3)cos(t)$ | $(9r^2 - 3)sin(t)$ | $1/\sqrt{6}$ |
| 3, 1 | 11 | curl | $(3r^2 - 3)sin(t)$ | $(9r^2 - 3)cos(t)$ | $1/\sqrt{6}$ |
| 4, 0 | 12 | curl | 0 | $24r^3 - 16r$ | $1/\sqrt{16}$ |
| 5, 1 | 13 | curl | $(10r^4 - 15r^2 + 5)sin(t)$ | $(50r^4 - 45r^2 + 5)cos(t)$ | $1/\sqrt{10}$ |
| 5, 1 | 14 | curl | $-(10r^4 - 15r^2 + 5)cos(t)$ | $(50r^4 - 45r^2 + 5)cos(t)$ | $1/\sqrt{10}$ |
| 6, 0 | 15 | curl | 0 | $120r^5 - 144r^3 + 36r$ | $1/\sqrt{24}$ |

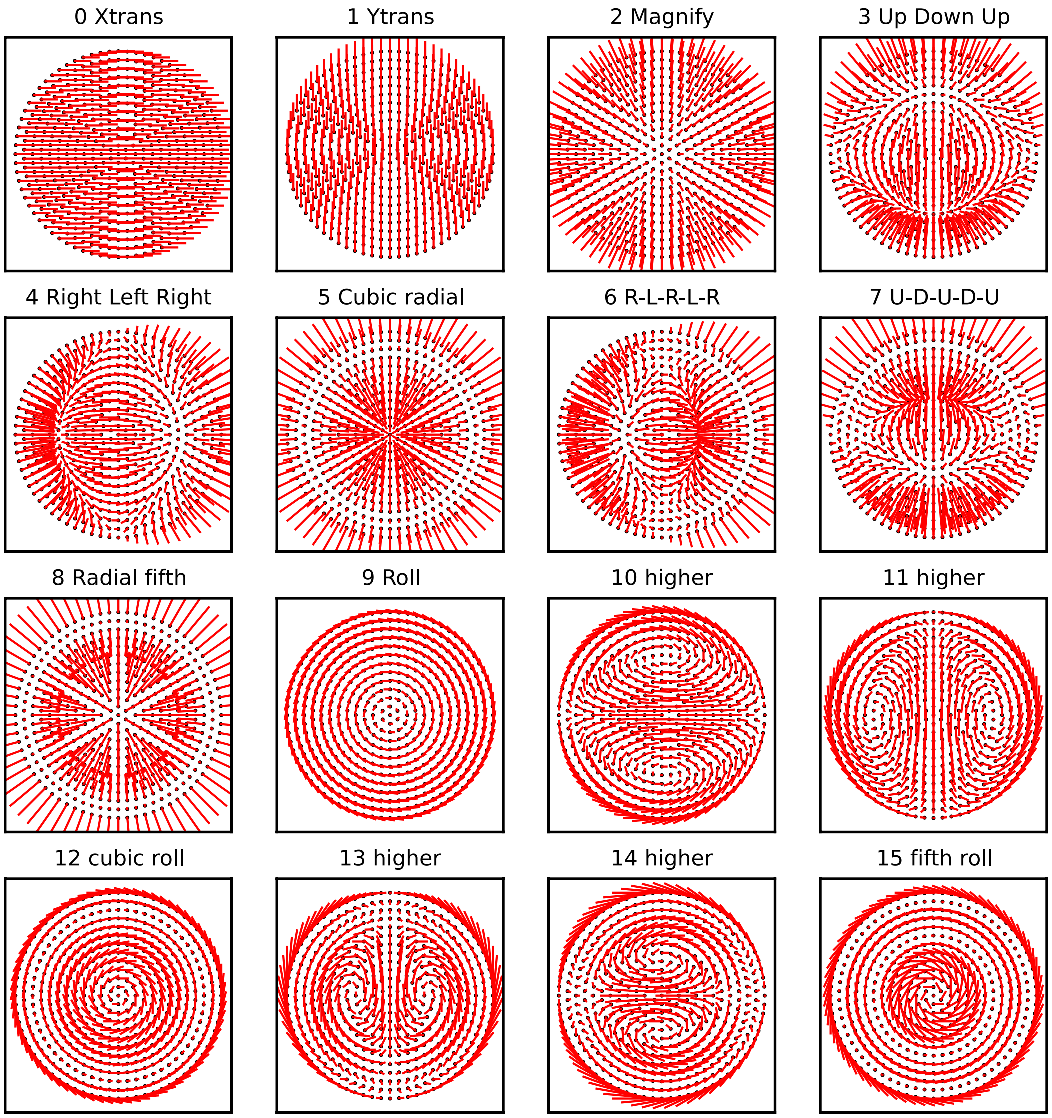


Figure 3: The sixteen vector fields from Table X plotted in the unit circle. These can be combined, as needed, to mimic a given distortion field. Each box title is the running index number used in this writeup and a descriptive phrase.

## 3 Results for DESI Distortion

If a vector distortion model is to be useful, it must span the space of optical distortions encountered on the job, giving good quantitative interpolation accuracy when fit to a collection of fiducial inputs. In this section I explore this accuracy.

### 3.1 Ideal Case, ADC=0, 120 Fiducials, Zero Fiducial Location Errors

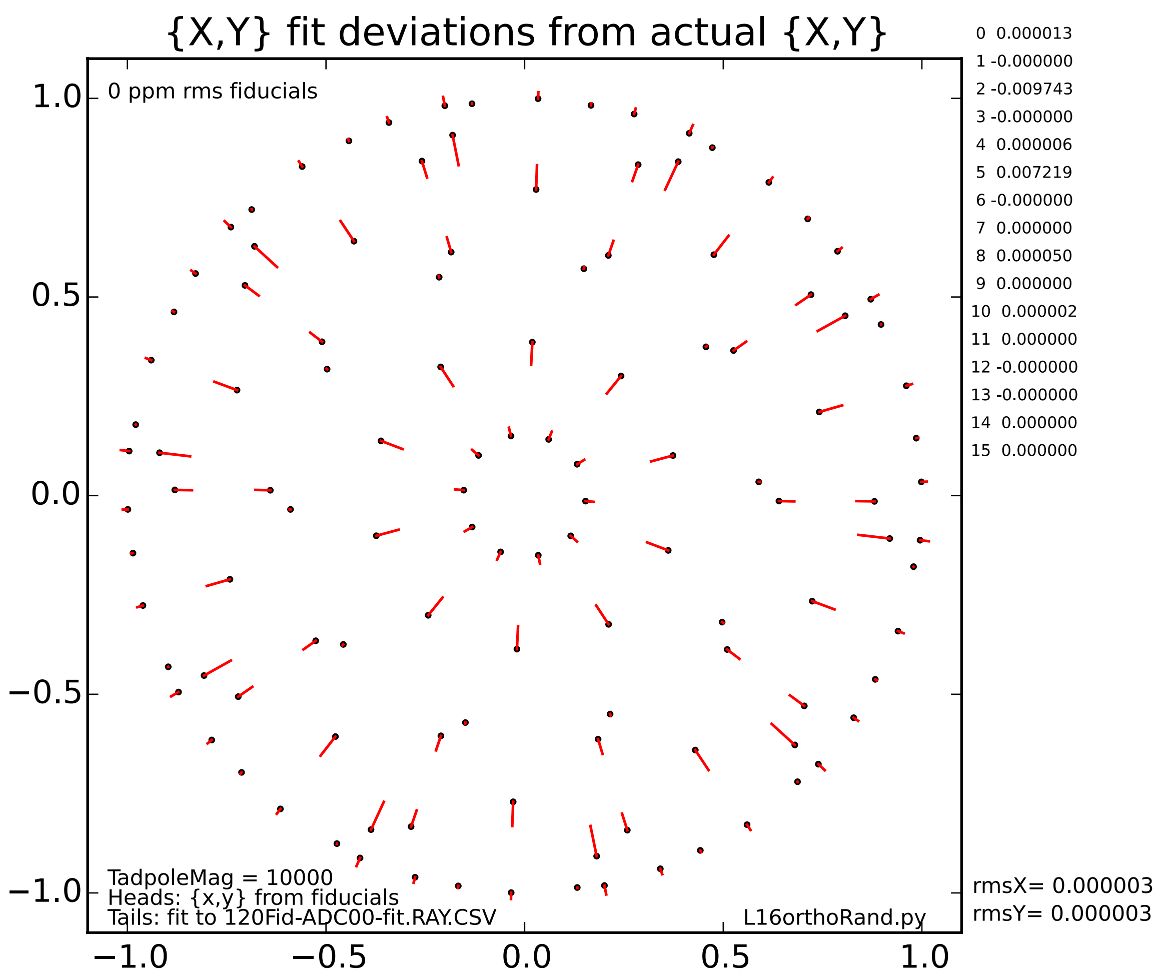


Figure 4: Here is the easiest case. An ideal E-22 corrector, perfectly aligned, ADC=0 degrees, was used to fit the 16 coefficients listed here at the 120 fiducial locations shown. The observed RMS fit errors are 3 ppm in x and y; they are perfectly radial although of high degree. On our 410mm radius focal plane, 1 ppm is 0.41 $\mu m$. Here, the tadpole magnification = 10000.

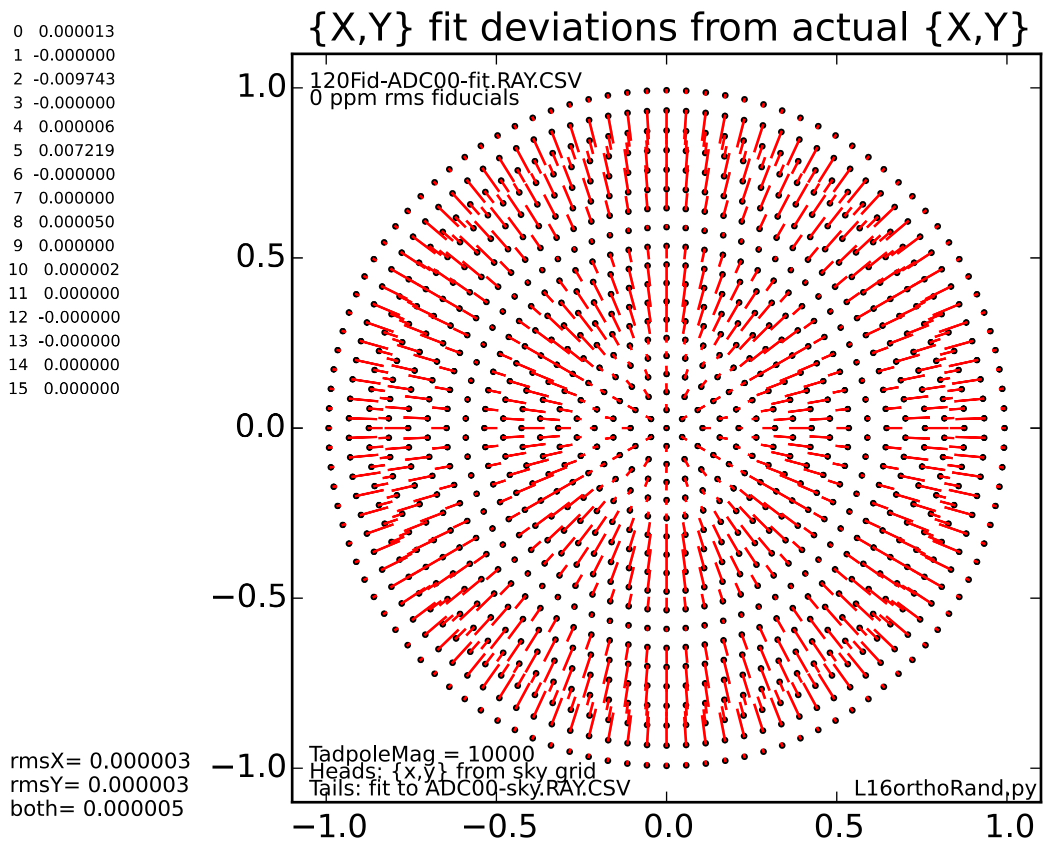


Figure 5: Here that coefficient set obtained in Figure 4 is used to interpolate a regular grid of 1027 sky locations. The RMS sky interpolation errors are again 3ppm each axis. Again the tadpole magnification = 10000.

## 3.2 Mangled Corrector120 Fiducials, Zero Fiducial Location Errors

A circularly symmetric optic will exhibit only the simplest kind of distortion, namely radial. With actual optics, asymmetries are introduced from many causes. In DESI, we have a symmetry-breaking atmospheric dispersion prism pair, and an overall collection of individual optical fabrication and mounting deviations, and finally large scale deviations due to hexapod motion, telescope bending, etc. So, it is important to stress test an interpolator by introducing serious asymmetries. The optic "Mangled8" used here provides such a test. The fit remains acceptable, about 4ppm (1.6 microns in the focal plane) for each axis.

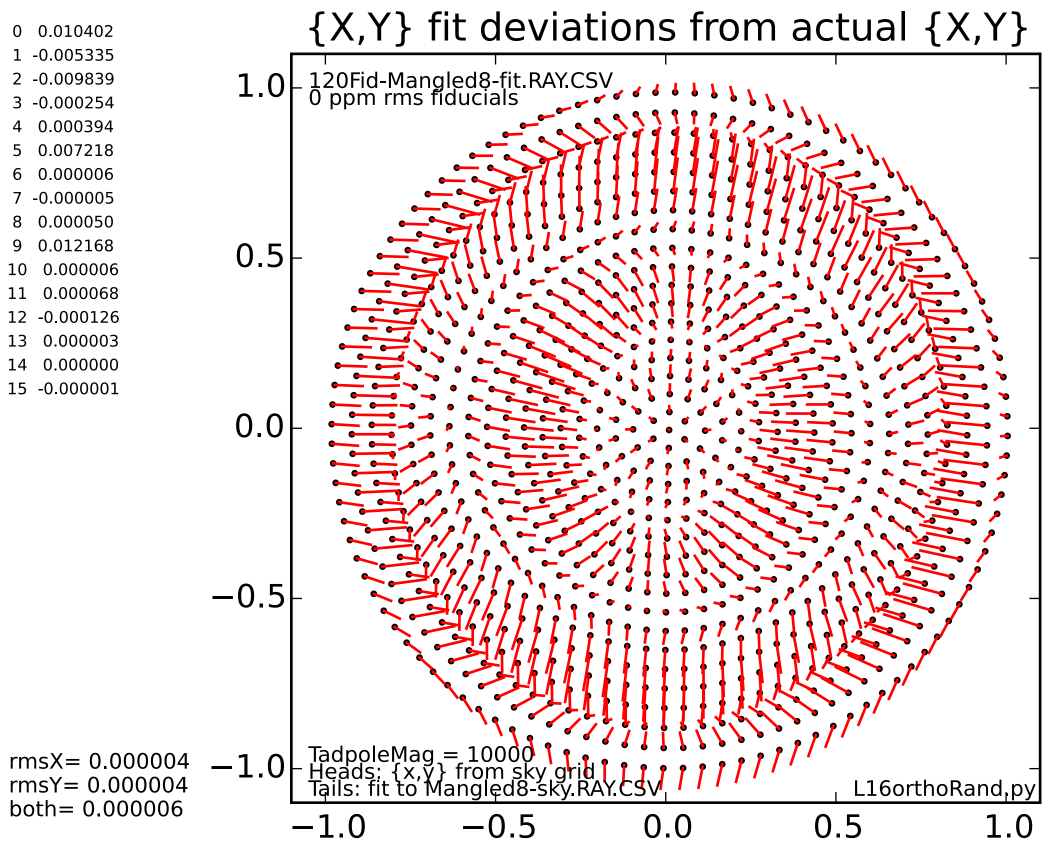


Figure 6: Here a seriously mangled corrector was created: each lens surface was offset by 0.1mm in X or Y or both, and each surface is tilted by 0.01 degrees in tilt or pitch or both. The entire hexapod is mis-centered by 1mm, and its axis no longer lies on the PM axis. This shows a noiseless fit to the 120 fiducials, and sky interpolation errors are plotted on our grid of 1027 sky points. The RMS fit errors rise slightly to 4 ppm in x and y. Again the tadpole magnification = 10000.

## 3.3 Now with Huge Random Position Errors on Fiducials

When many data samples together control a smaller number of adjustable fit parameters, we expect an error reduction to take place provided that the parameters are orthogonal. For DESI we have $N_c = 240$ constraints (120 on x, 120 on y) well distributed over the field, and with the present $N_p = 16$ parameters we can expect an error reduction factor of the order of $\sqrt{15}$ which is a roughly fourfold improvement. One run example is shown in Figure 7 below.

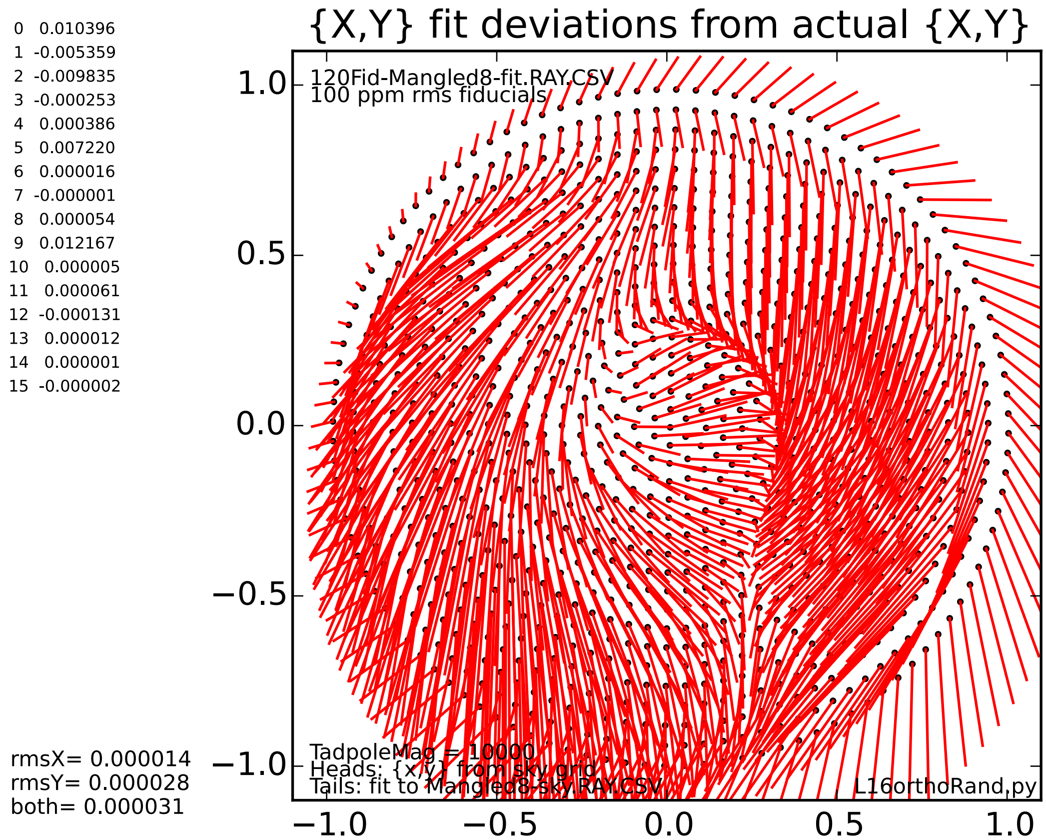


Figure 7: Mangled8 corrector with 100 ppm Gaussian random errors on each fiducial x and y. This run is typical, but the fit errors are jumpy: successive runs give values whose RMS is 20 to 30 ppm. Tadpole magnification = 10000.

To gather statistics of this error reduction process, I ran a sequence of 100 successive fitting runs with statistically independent Gaussian fiducial errors of 100 microns RMS in x and in y. My results are shown in Figure 8 below. The RMS 1D interpolation errors are 28ppm, i.e. about one quarter of the RMS fiducial errors.

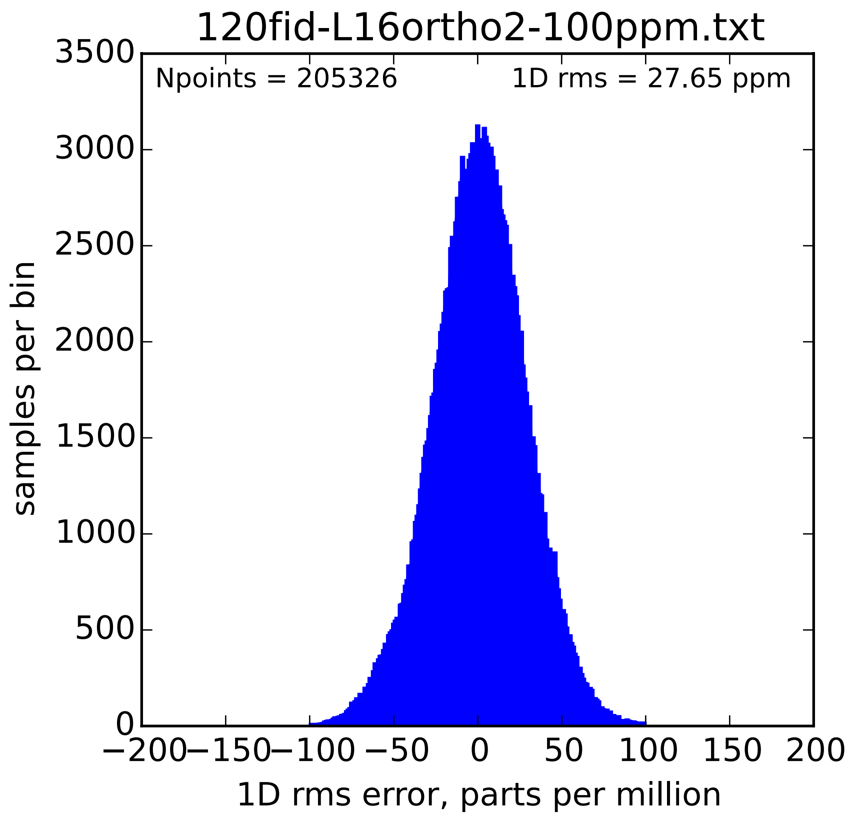


Figure 8: Distribution of interpolation errors with 120 fiducials (240 constraints) and 100ppm Gaussian errors in x and y for each fiducial. 16 parameters were fit. With fiducial errors this large, their statistics dominate the systematics, and we expect $e_i = e_f \sqrt{N_p/N_c}$ which is 26ppm, close to the observed 28ppm.

# 4 13 Parameters?

In the above lists of best fit coefficients, the final few coefficients remain small, with values of the order of a few ppm. I ran some experiments using the 13 most significant parameters and find that the fitting process accommodates the Mangled8 corrector systematics just about as well as the full sixteen parameter model, and has slightly improved fiducial error averaging.

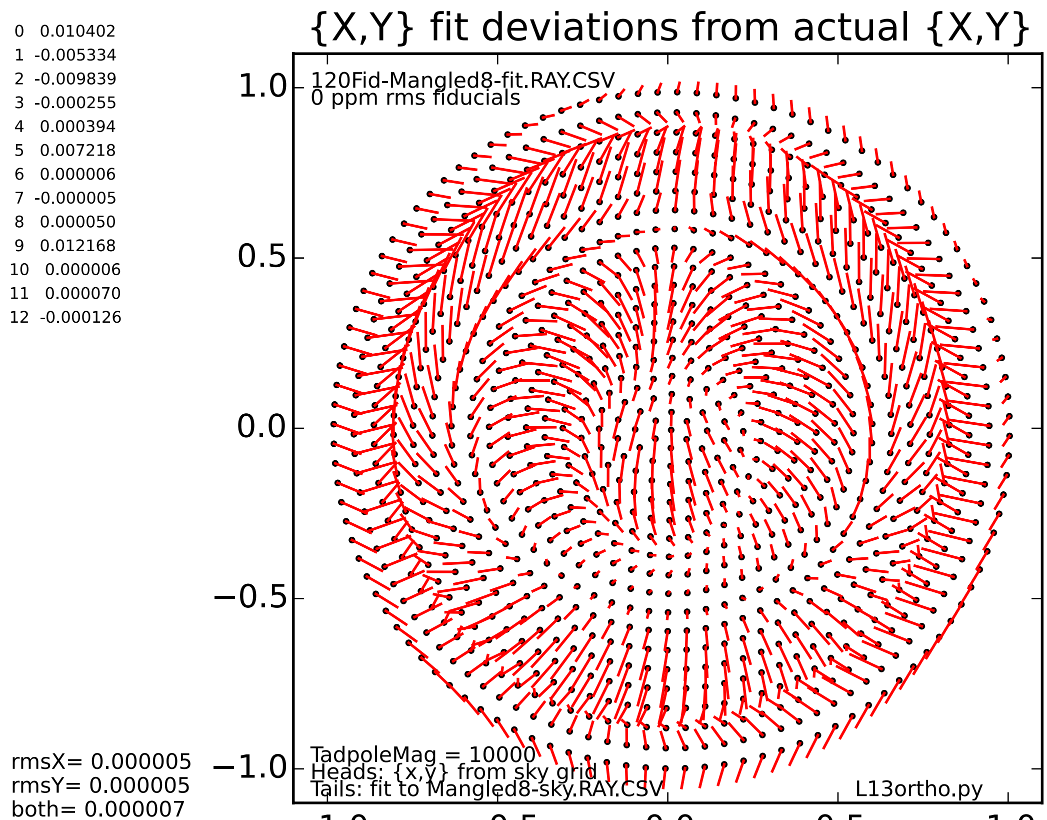


Figure 9: Like Figure 6, but now restricted to the top 13 parameters. Again I perform noiseless fit to the 120 fiducials, and sky interpolation errors are plotted on our grid of 1027 sky points. The RMS fit errors rise slightly to 5 ppm in x and y. Again the tadpole magnification = 10000.

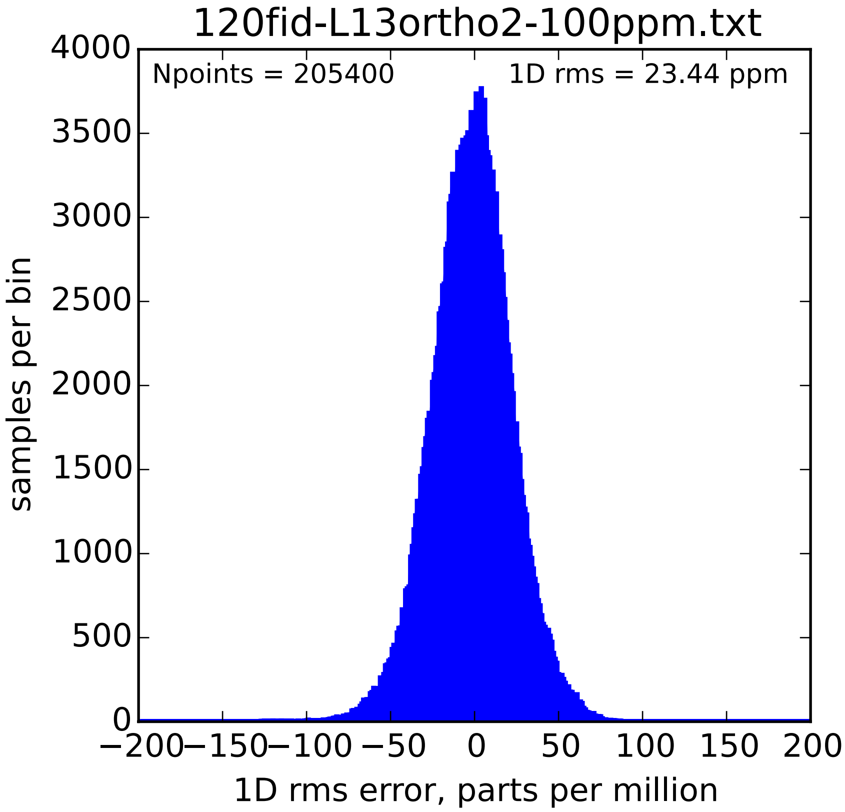


Figure 10: Distribution of interpolation errors with 120 fiducials and 100ppm Gaussian errors in x and y for each fiducial, but using only the top 13 parameters. This interpolator has slightly better error suppression compared to the 16 parameter model, as expected from $e_i = e_f \sqrt{N_p/N_c}$ .

## 5 Commissioning Instrument with 22 Fiducials

For initial commissioning, DESI will carry its full complement of corrector optics, but will not have 120 fiducials to monitor its distortion (120 fiducials is 240 mathematical constraints on twelve unknown interpolation coefficients). Instead, a smaller number of fiducial illuminators will be supplied. To explore the interpolator performance with fewer fiducials, I have run some cases with 22 fiducials, whose locations are defined by DESI-3115.

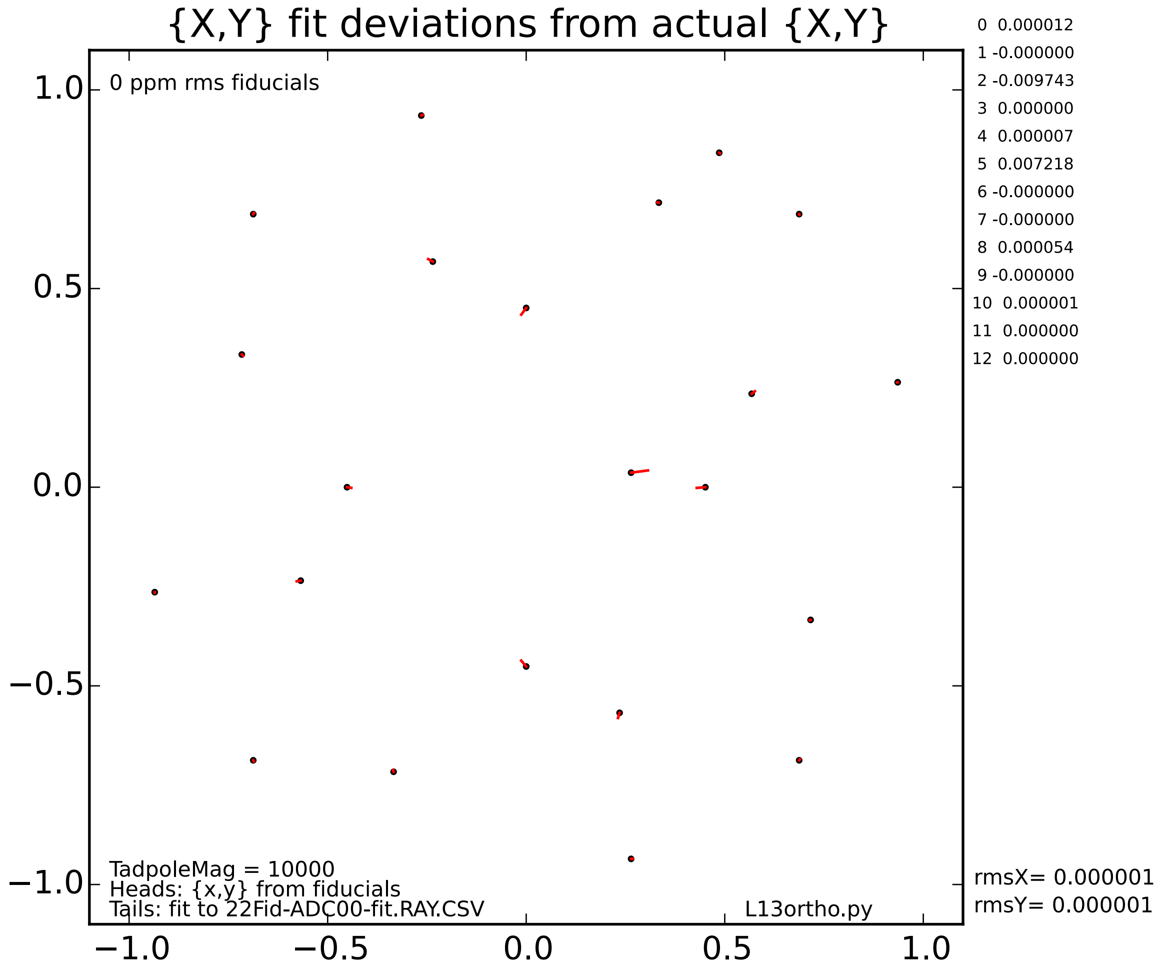


Figure 11: Excellent fit for the 22 fiducials using 13 parameters on an unperturbed optic.

From this brief study (see charts below), it appears that the benefit of using a large number of fiducials is to better average out fiducial placement metrology errors and fiber-view camera centroiding errors.

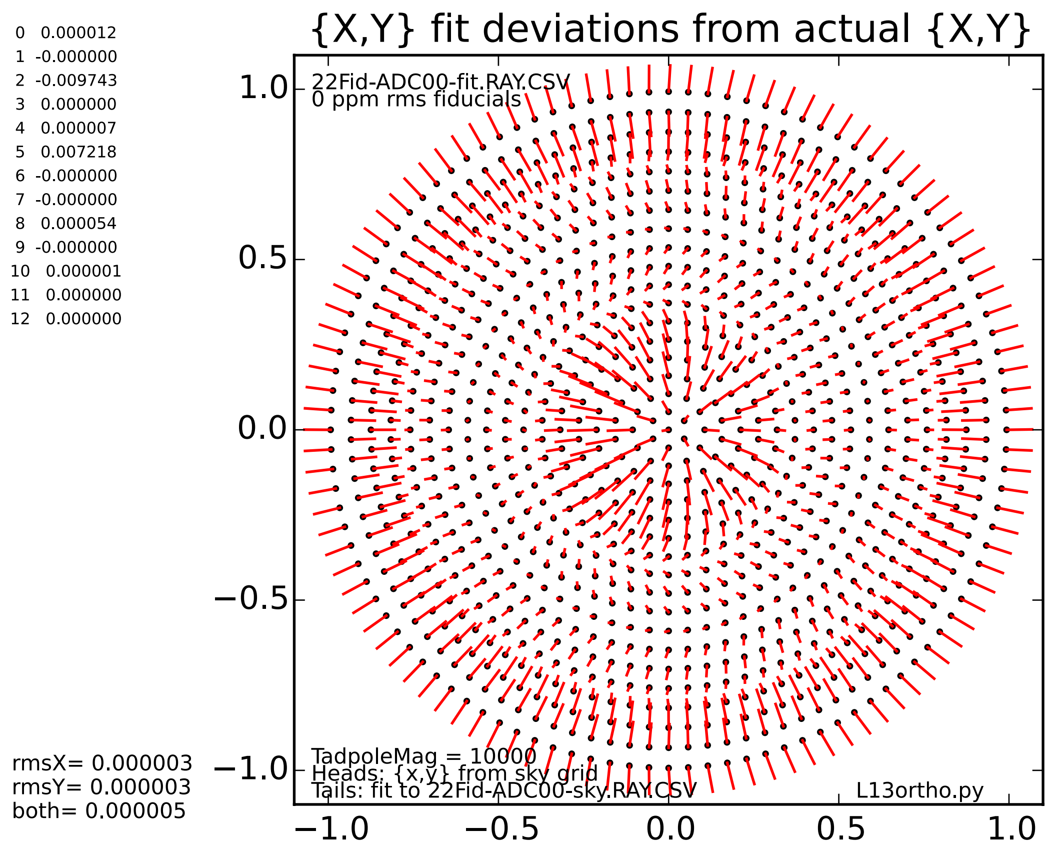


Figure 12: Sky interpolation with the parameters fit to this ideal case. Interpolation errors are just a few ppm over the full field.

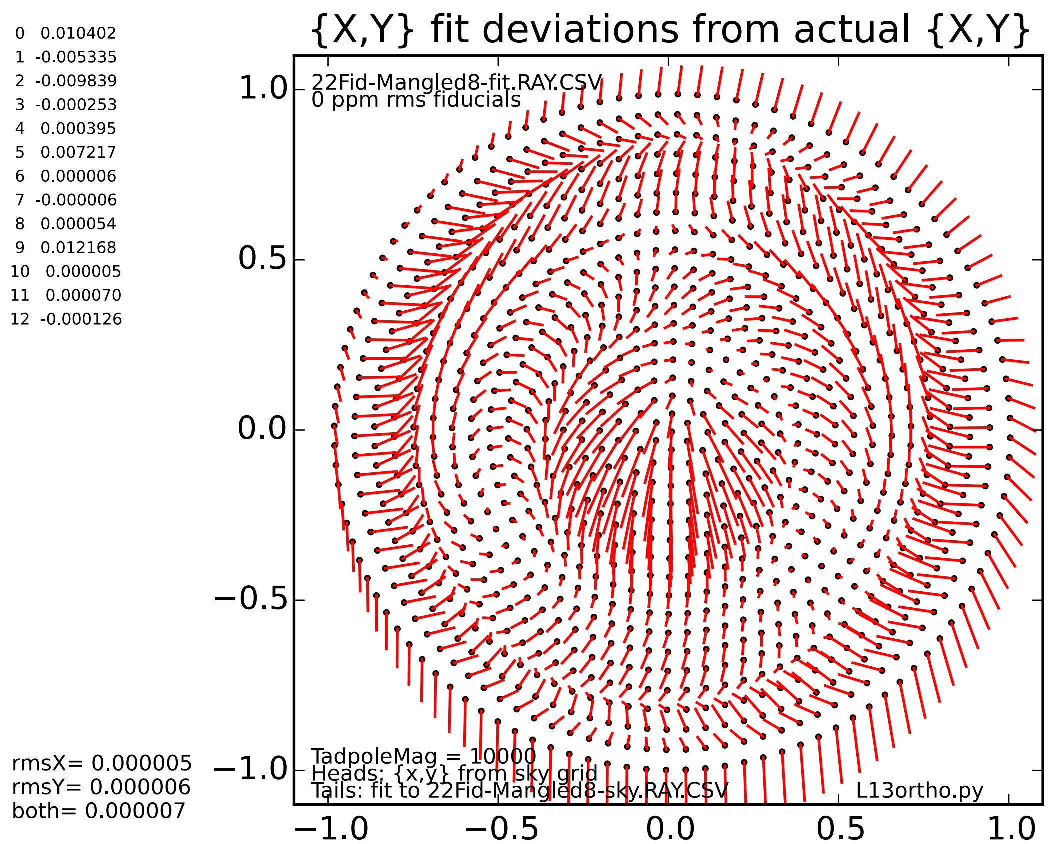


Figure 13: Sky interpolation with the parameters fit to the Mangled8 case. Zero fiducial location errors; interpolation errors increase slightly over the full field compared to the unperturbed optic situation.

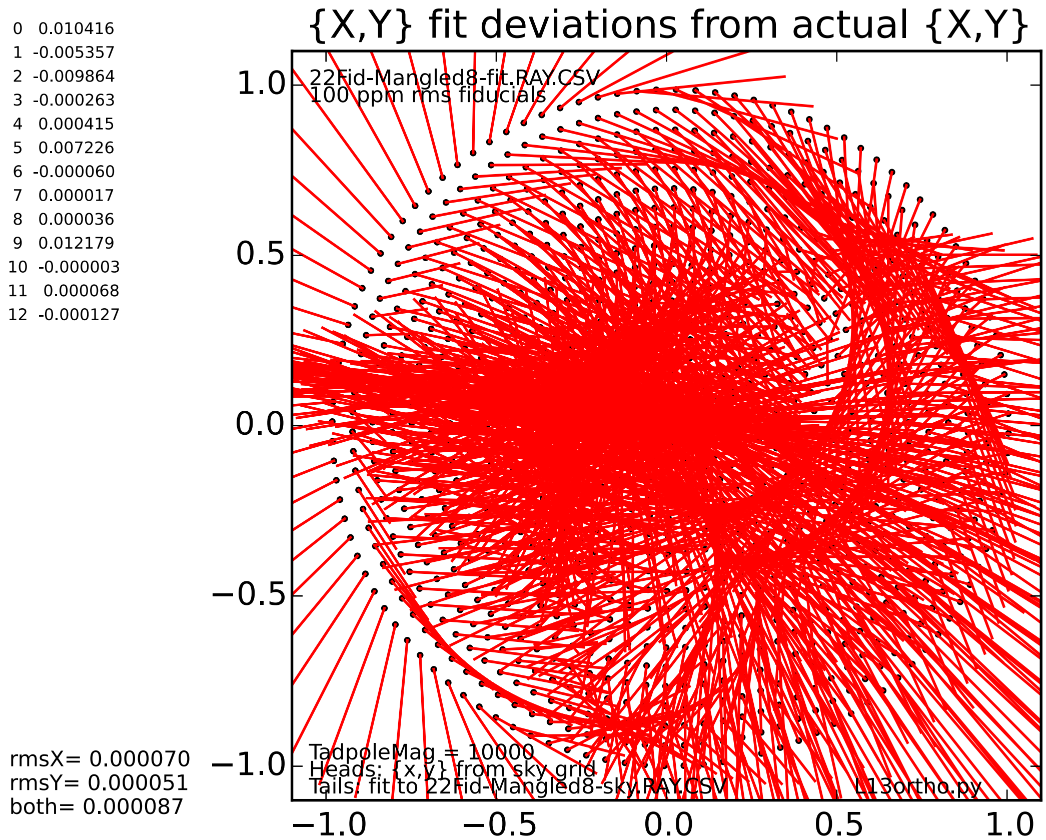


Figure 14: Sky interpolation with the 22 fiducials fit to the Mangled8 case. Input was 100 ppm fiducial location errors; resulting interpolation errors are much higher than for the full complement of 120 fiducials.

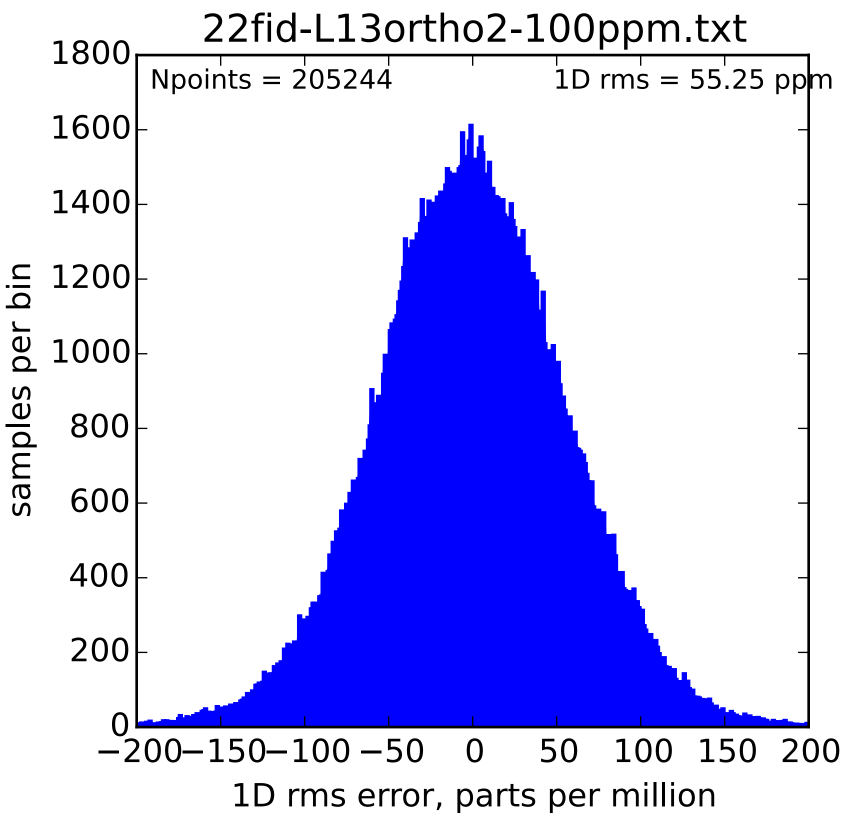


Figure 15: Distribution of interpolation errors with 22 fiducials and 100 ppm Gaussian input errors in x and y for each fiducial. The fit used only the top 13 parameters. Interpolation errors are 55ppm RMS, as expected from $e_i = e_f\sqrt{N_p/N_c}$ with 13 parameters and 44 constraints from the 22 fiducials.

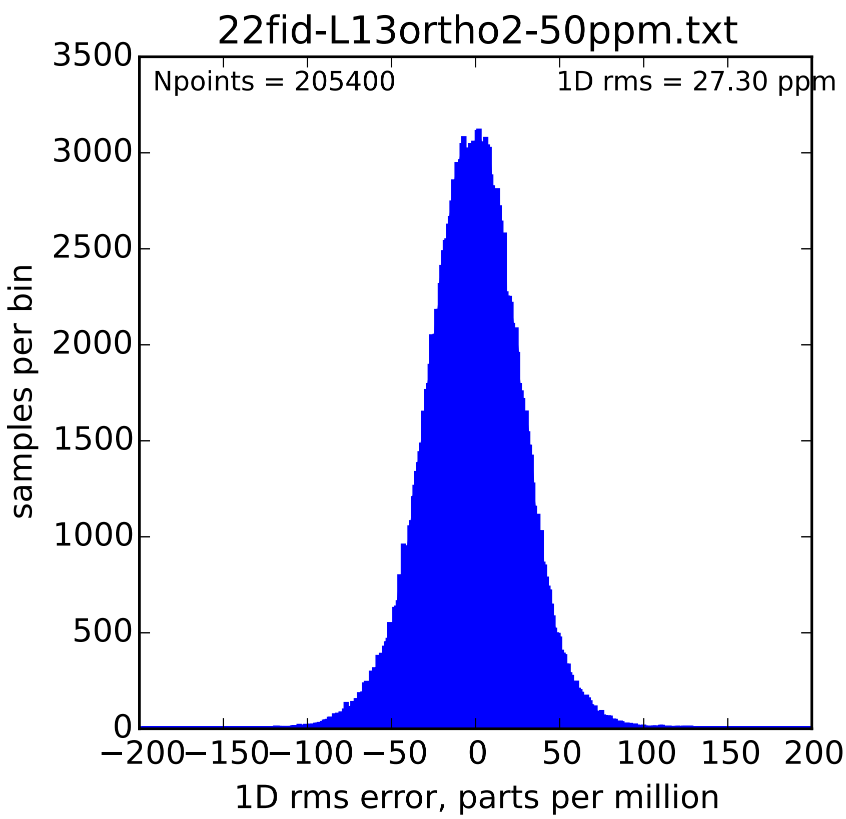


Figure 16: Distribution of interpolation errors with 22 fiducials and 50ppm Gaussian errors in x and y for each fiducial. The fit used only the top 13 parameters. Again the interpolation errors are about as expected.

# 6 Conclusions

1. **Systematic:** My distortion models using 16 and 13 parameters both have adequately small systematic errors, about 3 to 5 ppm ( 1 to 2 microns RMS in each axis).

2. **Random:** When fiducial location errors are large enough to dominate, either from their metrology or from their fiber-view camera centroids, the 120 fiducial case has superior averaging compared to the commissioning instrument's 22 fiducial case. Thanks to the orthogonality of the basis fields, In both cases the interpolation errors behave as expected for random independent constraints, namely $e_i = e_f\sqrt{N_p/N_c}$.